Meas. Sci. Technol. **19** (2008) 094001 (8pp) doi:10.1088/0957-0233/19/9/094001

Sub-micron resolution CT for failure analysis and process development

M Feser, J Gelb, H Chang, H Cui, F Duewer, S H Lau, A Tkachuk and W Yun

Xradia Inc., 5052 Commercial Circle, Concord, CA 94520, USA

E-mail: mfeser@xradia.com

Received 8 January 2008, in final form 10 June 2008
Published 24 July 2008
Online at stacks.iop.org/MST/19/094001

Abstract

Many modern industrial processes and research applications place increasingly higher demands on x-ray computed tomography (CT) imaging resolution and sensitivity for low-contrast specimens with a low atomic number. The three approaches to increasing imaging resolution are (1) reduction in the x-ray spot size, (2) use of higher resolution detectors or (3) employment of x-ray optical elements. Systems that pursue one or more of these approaches are available and under continued development. The Xradia MicroXCT™ projection-type microscope described in this paper has been optimized for high-resolution x-ray CT by employing a high-resolution detector paired with a microfocus x-ray source. Large working distances in this CT system enable full tomographic data collection at micrometre resolution of large samples, such as flip-chip packages. X-ray CT instruments using x-ray optical elements for condenser optics and imaging objective lenses are a new development capable of reaching sub-50 nm resolution. These instruments find various applications, including die-level imaging in the semiconductor industry as well as the process development for fuel cells, which we describe here as one application. Sub-micron resolution CT instruments without x-ray optical elements have a large application base already; however, new instruments optimized for soft materials and low-contrast specimens, such as the Xradia nanoXCT™, offer completely new capabilities and open new applications. New developments in the area of phase contrast imaging enable unprecedented image contrast for specimens with very low absorption, which for research applications enables for the first time the imaging of many specimens in their natural state (e.g., arteries to examine calcification). Zernike phase contrast for sub-50 nm x-ray CT even enables the imaging of single cell or thin tissue slices for biological or medical applications.

Keywords: x-ray microscopy, zone plates, x-ray optics, x-ray CT, Zernike phase contrast

(Some figures in this article are in colour only in the electronic version)

1. High-resolution CT based on projection imaging

Until very recently, all commercial x-ray computed tomography (CT) systems using laboratory sources were based on the principle of point projection of an x-ray source through the sample onto a detector. In this projection scheme, the achievable resolution is a function of both the x-ray source size and the detector resolution. Commonly, the resolution is thought to be driven by the x-ray source spot size. Figure 1 illustrates the geometric configuration of the projection-type x-ray microscope, where high resolution is achieved by magnifying the object onto the detector. Note that, as the distance between the source and object gets smaller, the magnification increases. At the same time, however, so does the blur in the detector plane r_s induced by the size of the source spot S. This blurring is given by

$$r_S = S\left(\frac{b}{a}\right) \tag{1}$$

where S is the size of the x-ray spot, a is the source to object distance and b is the object to detector distance. The resolution

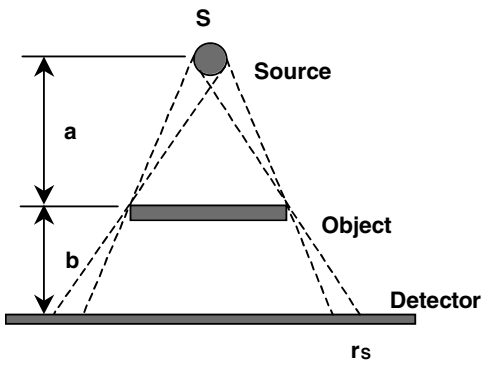

Figure 1. Illustration of geometric blurring due to the extended source size.

in the object plane may be calculated by dividing by the geometric magnification M, given by

$$M = \frac{a+b}{a}. \tag{2}$$

The blurring caused by the size of the x-ray source is commonly referred to as geometric unsharpness or penumbra. Due to the dependence of the system's resolution on both the source spot size and the resolution of the detector, the resolution of a projection-based x-ray microscope can be approximated by a convolution of the detector resolution and the source spot size, scaled by the geometric magnification:

$$r_{\text{total}} = \frac{\sqrt{r_D^2 + r_S^2}}{M} \tag{3}$$

(where r_D is the resolution of the detector system and r_S is the blurring due to the geometric unsharpness).

For many conventional x-ray projection-based systems, the resolution of the detector system is typically about 120 μm. To achieve high system resolution, the object must be placed very close to the source so that its projection is highly magnified onto the detector. Consequently, the x-ray source spot must be very small to achieve minimal geometric unsharpness and, thus, high system resolution. The highest achievable resolution for these systems is limited by both the spot size and the closest distance that can be allowed between the source and the sample. As a consequence, high-resolution projection x-ray systems use transmission-type sources to achieve a small source spot while minimizing the distance between the source and the sample. However, the proximity of the sample to the source severely restricts the size of the sample that can be imaged for tomography. For extended samples, the source-to-sample distance has to be increased, which will lead to a decreased system resolution. In addition, sub-micron imaging using transmission x-ray sources in magnifying geometry requires x-ray spot motion with magnitude less than the required imaging resolution, which is technologically challenging due to source instabilities and thermal drifts typical at high power loading.

As the detector resolution increases, however, equation (3) suggests that the source spot size is no longer a limiting factor for the system resolution. In other words, by using a high-resolution x-ray detector, a system resolution better than the

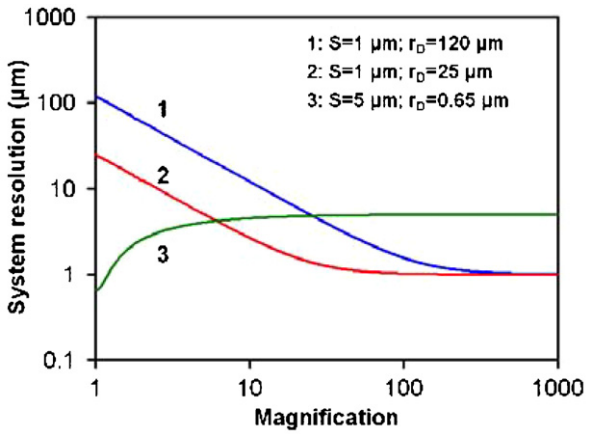

Figure 2. System resolution as a function of geometric magnification with different source spot sizes and detector resolutions.

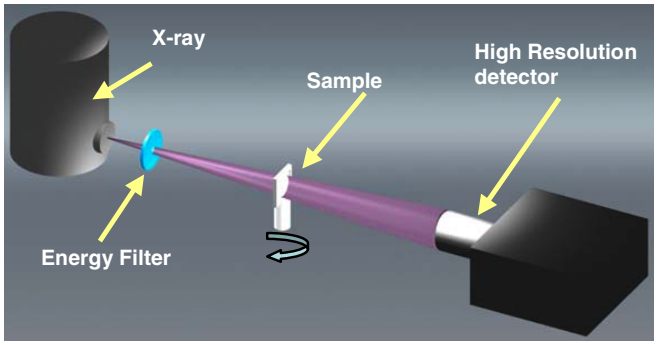

Figure 3. The Xradia MicroXCT uses a microfocus x-ray source with variable acceleration voltage up to 150 kV. The sample can be translated in x–y–z–theta directions on a high-resolution stage. High-resolution imaging is achieved using a 2048 × 2048 pixel CCD detector paired with lenses of varying magnification coupled to scintillating crystals, producing an effective detector pixel size <1 μm [14].

x-ray source spot size can be achieved even though the source spot size is larger than the detector resolution. The Xradia MicroXCT system is therefore capable of achieving 1 μm resolution by employing an x-ray detector with sub-micron resolution combined with a micro-focus x-ray source. This is illustrated by curve 3 in figure 2, in which the source spot size is 5 μm and the detector resolution 0.65 μm. In this system, working distances between source, sample and detector are typically around 100–150 mm, so full tomography can be achieved even for larger samples. The basic layout of the system is shown in figure 3.

One major application area of the Xradia MicroXCT system is failure analysis of IC packages. For this application, the relaxation of the sample-to-source minimum distance is crucial both for high-resolution imaging and collection of full tomography sets. For an advanced package structure (typically, from 12 mm × 12 mm × 2 mm up to 60 mm × 60 mm × 2 mm), it is clear that it will be difficult to simultaneously satisfy both the requirement from a resolution standpoint of placing the sample in near contact with the x-ray source and for tomographic data collection where it is

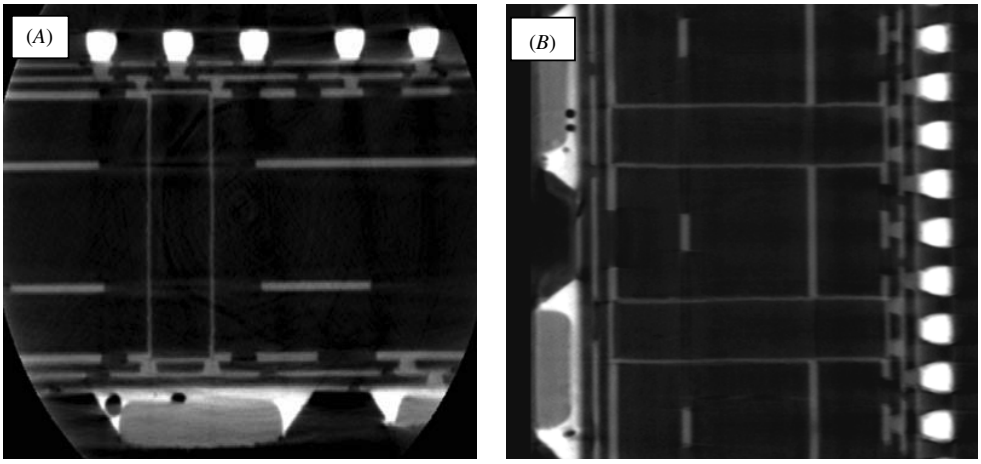

Figure 4. Lower resolution non-destructive tomographic cross-sections through the *XZ* plane (*A*) and *YZ* plane (*B*) of the 3D reconstruction of a flip-chip package. The controlled collapse chip connection (C4) layer is at the top of (*a*) and the pin connections to the socket can be seen at the bottom of the image. The plated through holes and copper inter-connects in the package are clearly visible. Resolution of this reconstruction is approximately 5 μm.

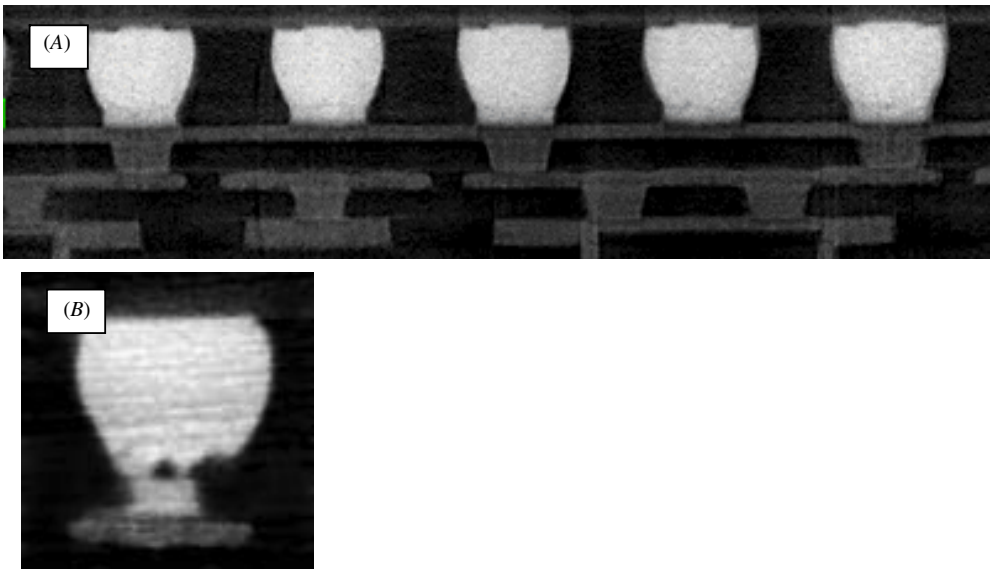

Figure 5. High-resolution non-destructive tomographic cross-sections through the reconstructed 3D volume of a flip-chip package showing details of the C4 solder bump connections. Resolution is approximately 1 μm (*A*). Non-destructive tomographic cross-section through failed C4 solder bump (*B*). Reconstruction is performed using a cone-beam back-projection algorithm on images taken over an angular range of 180° [7].

necessary to acquire at least 180° of data around the object. In a conventional projection-based x-ray microscope, it will be impossible to rotate the sample to such angular extremes without interfering with the x-ray source housing. One can move the sample further away from the x-ray source, however, but only at the expense of system resolution (as shown in figure 2).

As an example, we are showing a flip-chip microprocessor package. This sample was selected for its multi-layer complexity containing copper vias, plated through-holes and controlled collapse chip connections (C4) to the silicon die. The data were collected using the Xradia MicroXCT tomographic x-ray imaging system and represent 721 projection images collected over an angular range of 180°. The total data collection time was approximately 2 h, and reconstruction was performed using a filtered cone beam back-projection algorithm [7]. Figure 4 illustrates the non-destructive tomographic cross-sections through the 3D reconstruction of the flip-chip package. Note that there are no blurring artefacts since the required 180° of data were collected on this sample while simultaneously maintaining high resolution. Figure 5 shows a cross-section through the 3D reconstruction with 1 μm resolution. Again, note that there are no inter-layer blurring artefacts common to systems that collect limited angle data. Figure 6 shows a volume rendering of the dataset.

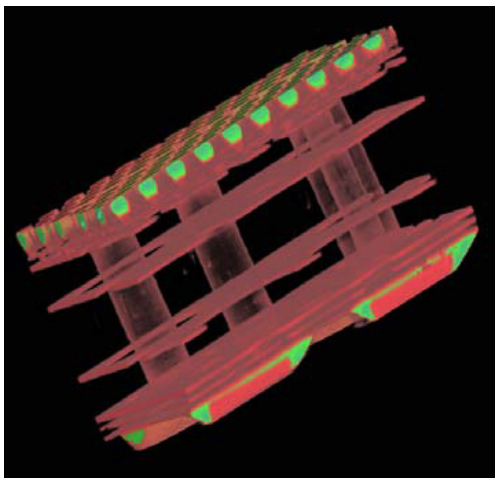

Figure 6. Volume rendering of a reconstructed 3D flip-chip package.

2. Nanoscale CT based on x-ray optics

2.1. Introduction

One of the approaches for x-ray nanoscale imaging is achieved with transmission x-ray laboratory sources through conventional x-ray point projection using a sub-micron spot size. Using this approach, 2D spatial resolution as fine as 0.25 μm has been reported for very thin samples. To obtain spatial resolution close to the spot size of the x-ray source, however, requires very large geometric magnification, which implies that the sample must be very close to the source. Because the specimen has to be rotated freely for tomography, spatial resolution using such point projection configuration degrades exponentially when the sample thickness and/or diameter is >1 mm. Coupled with the poor flux when an x-ray tube is operating with a small spot size, nanoscale x-ray imaging using this approach is not very practical.

Compared to a conventional point projection technique, Xradia's x-ray lens-based nanoXCT provides far superior spatial resolution (currently below 40 nm) and signal-to-noise ratio with optimized photon collection in a configuration similar in principle to high-resolution visible light and electron microscopy systems, as illustrated in figure 8 [13]. Incident x-rays, from either a laboratory or synchrotron source, are initially focused by a reflective capillary optic, designed to condense a selection of the rays to a small spot [15]. The sample is illuminated at this point, after which the rays begin to diverge. About 20 mm past the sample position, a diffractive focusing optic, called a Fresnel zone plate (figure 7), captures the diverging rays and focuses the transmission image of the sample several hundred millimetres downstream [9]. The x-rays are then converted to a visible light image by a scintillating crystal, and that image is finally captured by a high-resolution CCD detector, similar to the one described in section 1 [14].

Relative positions between sample, zone plate and detector naturally determine x-ray optical magnification, which is typically about 40×. Coupled with a 20× optical magnification in the detector, total system magnification is roughly 800×. Employing a 1024 × 1024 CCD detector with a physical pixel size of 13 μm, the effective pixel size becomes approximately 16 nm on the sample plane. The simple Rayleigh resolution δ of an x-ray microscope is a function of the outermost zone width Δr_n of the objective zone plate:

$$\delta = 1.22\Delta r_n. \tag{4}$$

Thus, the resolution of the zone-plate-based x-ray microscope is independent of the x-ray source spot size and is ultimately limited by the outermost zone width of the zone plate (finer zones give higher resolution). For a zone plate of the outmost zone width of 35 nm, the Rayleigh resolution of ∼42.7 nm may be theoretically obtained, which is oversampled three times by the detector in the geometry described. This resolution has been routinely achieved using the configuration described [12, 13].

While most of the x-ray microscopes installed at synchrotron radiation facilities use soft x-ray energies [1–3], the Xradia nanoXCT system uses x-ray energies between 5 and 15 keV produced by either table-top or synchrotron sources [13]. One of the advantages of using higher x-ray energies is to provide greater penetrating power and depth of focus (DOF), which is a function of x-ray wavelength and the numerical aperture (NA) of the focusing optic:

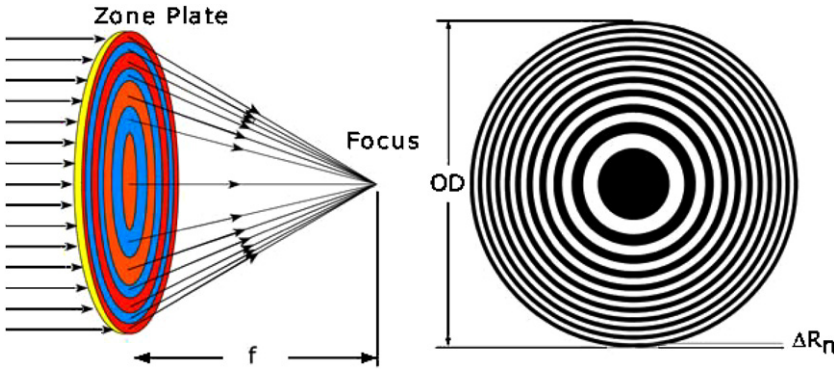

Figure 7. Fresnel zone plates as focusing optics for x-rays. Rings ('zones') of various widths cause incident light to be diffracted at zone-dependent angles, causing a convergence (focusing) of the beam.

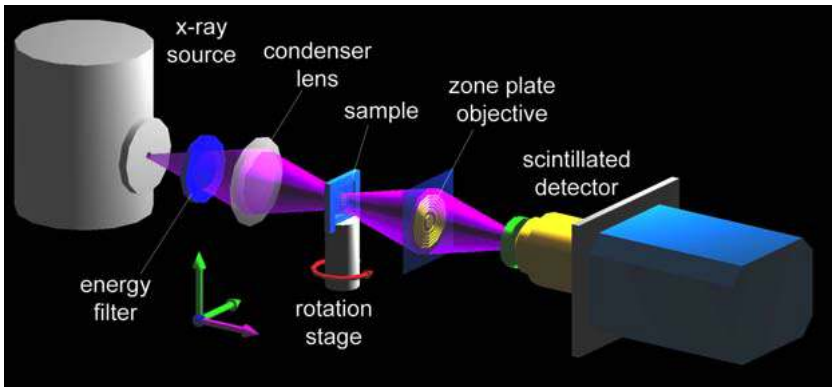

Figure 8. Schematic of the sub-50 nm resolution nanoXCT 3D x-ray CT system with reflective condenser, Fresnel zone plate optics and high-resolution imaging detector.

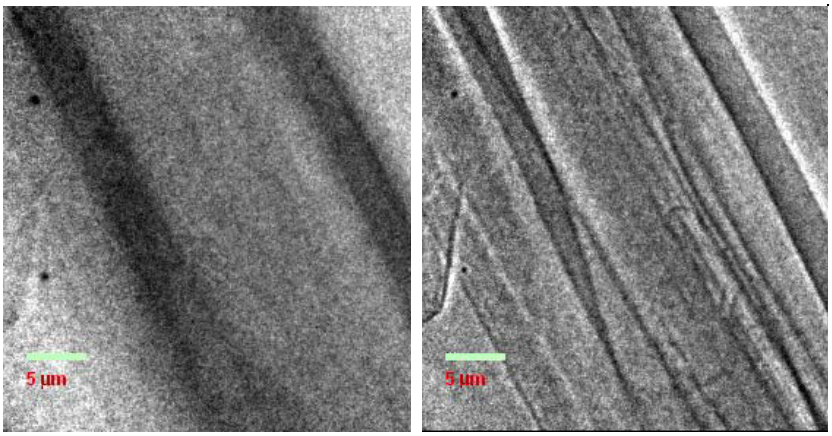

Absorption contrast (*a*) Phase contrast (*b*)

Figure 9. Wood imaged in absorption (*a*) and Zernike phase contrast (*b*) modes using a laboratory nanoXCT system in large field of view (∼50 × 50 um) mode with ∼150 nm resolution. Both (*a*) and (*b*) are x-ray images of the same region of interest. Sample courtesy of China's International Centre for Bamboo and Rattan [10].

$$\mathrm{DOF} = \pm\frac{\lambda}{2(\mathrm{NA})^2} = \frac{2\delta r^2}{\lambda}. \tag{5}$$

For example, the sample thickness requirements for tomography using soft x-rays is typically 1–3 μm, which is problematic for CT. At higher x-ray energies, such as 8 keV Cu Kα emission, the sample thickness that x-rays can penetrate is relaxed to 100 μm for materials with density similar to Si and a large DOF (∼50 μm) may be achieved (ideal for CT). TEM, by contrast, requires a sample thickness on the order of 10 nm–1 μm for very light samples (in the case of soft tissue with the high-voltage TEM operating at low magnification). Charged particle techniques from electron microscopy have other disadvantages, including the need for the sample to be conductive, the possible addition of contrast agents and the need for the sample to be vacuum compatible.

Conventional laboratory electron-impact x-ray sources with solid targets, using target materials such as Rh, Cr and Cu, generate characteristic photon energies at 2.7, 5.4 and 8.0 keV, respectively (zone plates require selection of one emission line for monochromaticity [9]). All those laboratory sources are in use in the Xradia nanoXCT setup, and 7–14 keV x-ray energies are in use in the synchrotron-based nanoXCT-S systems [13]. By rotating the specimen on an ultraprecision stage, tomography projections of specimens up to 100 μm thick with a 20 μm × 20 μm field of view may be obtained at sub-50 nm resolution at 8 keV x-ray energy, or 30 nm resolution at 2.7 keV energy.

Xradia has recently increased the x-ray throughput of the nanoXCT system while maintaining sub-50 nm resolution by doubling the aspect ratio of the zone plates in use. Though conventional manufacturing techniques have limited the achievable aspect ratio for small zone sizes in the past, Xradia has developed a technique that overcomes these issues. Details of this process are presented elsewhere [11].

2.2. Image contrast in Xradia's nano-CT systems

Image contrast in transmission x-ray imaging is mainly based on absorption differences between different materials within the sample. For many materials at high x-ray energies, the x-ray attenuation length can be very long, resulting in little x-ray absorption and therefore poor imaging contrast. To overcome this problem, the Xradia x-ray microscope can dramatically increase imaging contrast by operating in the

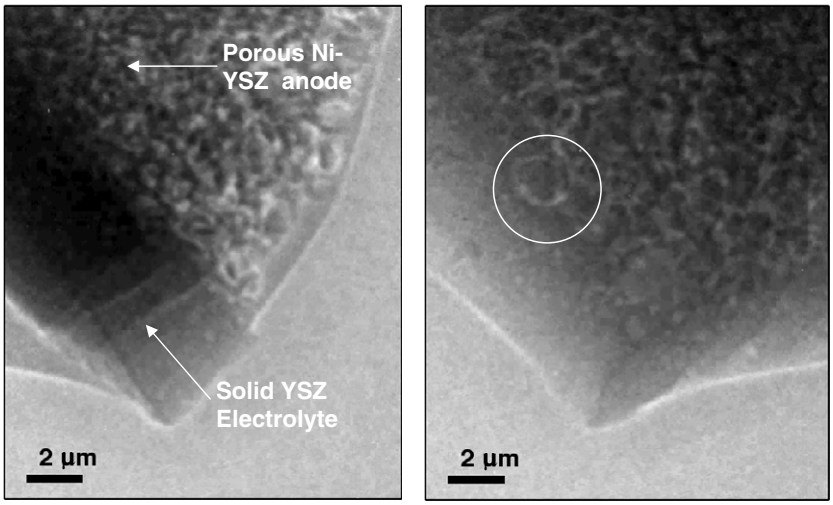

Figure 10. Raw projection data produced by the x-ray CT system operating at 8 keV in Zernike phase contrast mode. 181 projections (only two are shown) were taken every degree from the -90° to $+90^\circ$ angular range. The grey-level image intensity is such that the denser and/or thicker the material, the darker it appears on the image. Solid YSZ electrolyte and porous Ni–YSZ anode are clearly distinguished on the images. The circled feature on the right image has been used as a reference in subsequent figures of the reconstructed volume. Data acquisition time was 5 min per 2D projection for a total of ∼900 min.

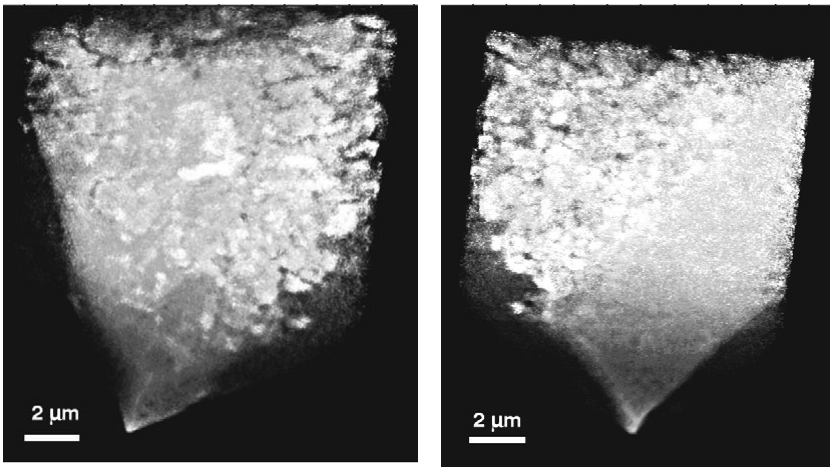

Figure 11. Volume rendering of the SOFC, reconstructed from 181 projections (see figure 10) taken over an angular range of -90° to $+90^\circ$. Note that the contrast is reversed compared to figure 10, e.g. the SOFC material appears in bright colour against black background (air).

Zernike phase contrast mode by means of inserting a phase ring into its optics train [12]. The phase ring is designed and manufactured to a precise thickness, such that it shifts the phase of the undiffracted (i.e. unfocused) light by $-3\pi/2$ rad. When the unmodified diffracted light recombines with the phase-shifted undiffracted light, their interference in the detector plane leads to contrast enhancement for some spatial frequencies, resulting in negative Zernike phase contrast [4, 5].

Figure 9 shows a comparison of a wood sample in both absorption and phase contrast. In both images, all acquisition and setup parameters are the same, except for the insertion of the phase ring in (*b*).

2.3. Example application

As an example of the application of the nanoXCT system, we show CT data of a fragment of a hollow tubular solid oxide fuel cell (SOFC) with a solid YSZ electrolyte shell and a much thicker porous Ni–YSZ anode layer on the inside [6, 12]. Two of the 181 collected raw 2D projection images are shown in figure 10. Each projection is imaged in phase contrast by a high-resolution x-ray detector (scintillator coupled to CCD detector) while rotating the sample in steps of 1° from -90° to $+90^\circ$, as schematically depicted in figure 8 [14]. Data collection is fully automated with an exposure time of 5 min per projection in order to obtain data with a good signal-to-noise ratio. Since the electron densities of the solid and porous material are very similar, the solid YSZ electrolyte appears darker on the left image because of the greater projected thickness through which x-rays had to penetrate at this particular imaging angle.

CT was performed to reconstruct the 3D volume of the object by applying a filtered parallel beam back-projection algorithm [7]. Hardware-accelerated software completes

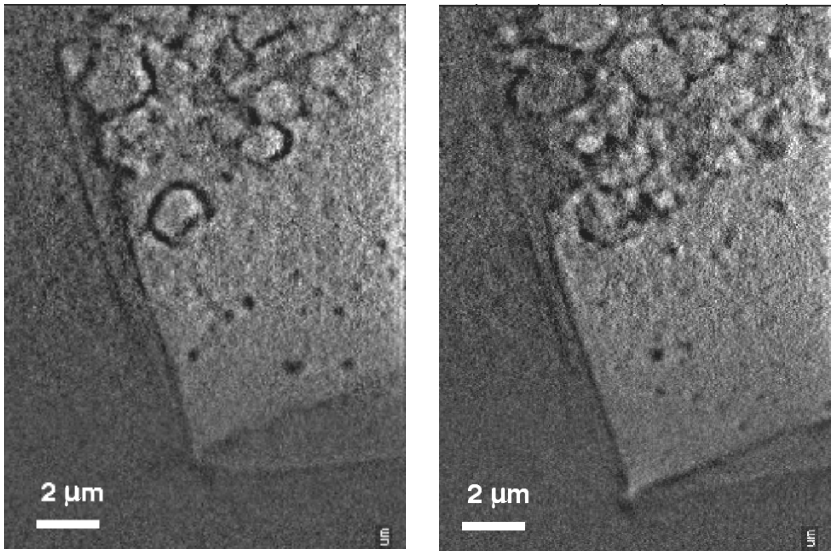

(*a*) (*b*)

Figure 12. Examples of two cross-sections ∼1 μm apart extracted from the reconstructed 3D volume shown in figure 11. Sub-100 nm pores (dark dots) are visible inside the solid YSZ electrolyte wall. Porosity and channels inside the porous Ni–YSZ anode are also clearly visible together with the PTB interface separating solid and porous regions.

reconstruction of the 512 × 512 × 512 pixel volume in ∼90 s. Snapshots of the reconstructed 3D volume of the SOFC fragment at two different rotation angles are shown in figure 11.

The reconstructed 3D volume of the SOFC fragment subsequently can be subjected to non-destructive tomographic cross-section and segmentation. Two cross-sections extracted from the 3D volume in figure 11 separated by ∼1 μm are shown in figure 12. These virtual layers clearly depict the solid YSZ electrolyte—Ni–YSZ anode interface, as well as nano-porosity and tortuosity, which are important for understanding the mechanisms responsible for optimizing the operating conditions of SOFCs that allow high performance and longevity. The ability to image these nano-porous structures in 3D to study the size, distribution and connectivity of the pores and channels is critical for speeding up the development and proliferation of SOFC technology. Detailed analysis and modelling based on the results of this work are currently underway and will be presented elsewhere [8].

3. Conclusions and outlook

For projection-type x-ray CT systems, we have shown that artefact-free micrometre-resolution tomographic imaging is possible by using a high-resolution x-ray detector, which poses a problem for conventional projection-based x-ray microscopes where the sample has to be located very close to the x-ray source. We have illustrated the advantage of this technology in the Xradia MicroXCT system for a flip-chip package, which has been imaged with a full 180° rotation dataset. Micrometre resolution is critical for the unambiguous identification and localization of failures in modern and future chip packages.

For nanoscale x-ray CT, we described the Xradia nanoXCT imaging system, which has a resolution of better than 50 nm at 8 keV and 30 nm at 2.7 keV. The practicality of the x-ray microscope is based on the development of high-performance, high-efficiency x-ray optical components. The example shown, a solid oxide fuel cell, demonstrates the power of the CT system to image internal nanoscale features of optically opaque and dense materials. In the future, the continued advancement in zone plate resolution and efficiency in the hard x-ray energy range promises even higher throughput and spatial resolution, since the resolution of the x-ray lens is currently only limited by fabrication capabilities. The development of novel laboratory x-ray sources and the utilization of high-brightness synchrotron sources will open new opportunities for faster, higher-resolution x-ray CT. It is expected that high-resolution CT using hard x-rays will proliferate into many areas of R&D and industrial applications as it bridges the gap between visible light and electron microscopy.

References

[1] Attwood D 2006 Nanotomography comes of age *Nature* **442** 642–3
[2] Chao W, Harteneck B D, Liddle J A, Anderson E H and Attwood D T 2005 Soft x-ray microscopy at a spatial resolution better than 15 nm *Nature* **435** 1210–3
[3] Kim K W *et al* 2006 Compact soft x-ray transmission microscopy with sub-50 nm spatial resolution *Phys. Med. Biol.* **51** N99–107
[4] Rudolph D, Schmahl G and Neimann B 1990 Amplitude and phase contrast in x-ray microscopy *Modern Microscopies. Techniques and Applications* ed A Michette and P Duke (London: Plenum) pp 59–67
[5] Zernike F 1935 Das Phasenkontrastverfahren bei der mikroskopischen Beobachtung *Z. Tech. Phys.* **36** 848–51
[6] Wilson J R, Kobsiriphat W, Mendoza R, Chen H, Hiller J M, Miller D J, Thornton K, Voorhees P W, Adler S B and Barnett S A 2006 Three-dimensional reconstruction of a solid-oxide fuel-cell anode *Nature Mater.* **5** 541–4

[7] Kak A C and Slaney M 1988 *Principles of Computerized Tomographic Imaging* (Piscataway, NJ: IEEE) pp 49–112
[8] Izzo J R Jr, Joshi A S, Peracchio A A, Grew K N, Chiu W K S, Tkachuk A T, Wang S H and Yun W 2008 Nondestructive reconstruction and analysis of solid oxide fuel cell anodes using x-ray computed tomography at sub-50 nm resolution *J. Electrochem. Soc.* **155** B504–8
[9] Young M 1972 Zone plates and their aberrations *J. Opt. Soc. Am.* **62** 972–6
[10] International Centre for Bamboo and Rattan. Available at http://www.icbr.ac.cn/
[11] Feng Y, Feser M, Lyon A, Rishton S, Zeng X, Chen S, Sassolini S and Yun W 2007 Nanofabrication of high aspect ratio 24 nm x-ray zone plates for x-ray imaging applications *J. Vac. Sci. Technol.* B **25** 2004–7
[12] Tkachuk A, Duewer F, Cui H, Feser M, Wang S and Yun W 2007 X-ray computed tomography in Zernike phase contrast mode at 8 keV with 50-nm resolution using Cu rotation anode X-ray source *Z. Kristallogr.* **222** 650–5
[13] Chu Y S *et al* 2008 Hard-x-ray microscopy with Fresnel zone plates reaches 40 nm Rayleigh resolution *Appl. Phys. Lett.* **92** 103119
[14] Koch A, Raven C, Spanne P and Snigirev A 1998 X-ray imaging with submicrometer resolution employing transparent luminescent screens *J. Opt. Soc. Am.* A **15–17** 1940–51
[15] Zeng X, Duewer F, Feser M, Huang C, Lyon A, Tkachuk A and Yun W 2008 Ellipsoidal and parabolic glass capillaries as condensers for x-ray microscopes *Appl. Opt.* **47** 2376–81